

Synthesis and characterization of trimetallic cobalt, zinc and nickel complexes containing amine-bis(benzotriazole phenolate) ligands: efficient catalysts for coupling of carbon dioxide with epoxides

Chen-Yu Li,^{a,d} Yu-Chia Su,^b Chia-Her Lin,^a Hsi-Ya Huang,^a Chen-Yen Tsai,^{*b} Ting-Yu Lee^{*c} and Bao-Tsan Ko^{*a,b}

^aDepartment of Chemistry, Chung Yuan Christian University, Chung-Li 32023, Taiwan

^bDepartment of Chemistry, National Chung Hsing University, Taichung 402, Taiwan

^cDepartment of Applied Chemistry, National Kaohsiung University, Kaohsiung 81148, Taiwan

^dTechnology Research Development, Plastic Industrial Development Center, Taichung 407, Taiwan

Table S1 Selected bond length (Å) and bond angles (°) for cobalt complex **1**

Table S2 Selected bond length (Å) and bond angles (°) for zinc complex **2**

Table S3 Selected bond length (Å) and bond angles (°) for nickel complex **3**

Table S4 Crystallographic data of complexes **1-3**

Fig. S1 ¹H NMR spectrum of the methine region of crude sample produced by coupling of cyclohexene oxide and CO₂ using cobalt acetate complex **1** in the presence of *n*-Bu₄NCl (5 mol%) at 80 °C and 300 psi CO₂ (400 MHz, CDCl₃).

Fig. S2 ¹H NMR spectrum of the crude sample from cycloaddition of **4b** and CO₂ using tri-cobalt acetate complex **1** in the presence of *n*-Bu₄NCl.

Fig. S3 ¹H NMR spectrum of the crude sample from cycloaddition of **4c** and CO₂ using tri-cobalt acetate complex **1** in the presence of *n*-Bu₄NCl.

Fig. S4 ¹H NMR spectrum of the crude sample from cycloaddition of **4d** and CO₂ using tri-cobalt acetate complex **1** in the presence of *n*-Bu₄NCl.

Fig. S5 ¹H NMR spectrum of the crude sample from cycloaddition of **4e** and CO₂ using tri-

cobalt acetate complex **1** in the presence of *n*-Bu₄NCl.

Fig. S6 ¹H NMR spectrum of the crude sample from cycloaddition of **4f** and CO₂ using tri-cobalt acetate complex **1** in the presence of *n*-Bu₄NCl.

Fig. S7 ¹H NMR spectrum of the crude sample from cycloaddition of **4g** and CO₂ using tri-cobalt acetate complex **1** in the presence of *n*-Bu₄NCl.

Fig. S8 ¹H NMR spectrum of the crude sample from cycloaddition of **4h** and CO₂ using tri-cobalt acetate complex **1** in the presence of *n*-Bu₄NCl.

Fig. S9 ¹H NMR spectrum of the crude sample from cycloaddition of **4i** and CO₂ using tri-cobalt acetate complex **1** in the presence of *n*-Bu₄NCl.

Fig. S10 Variable-temperature ¹H NMR spectrum (400 MHz) of tri-Zn complex **2** in CDCl₃ taken at different temperatures: (a) 25 °C; (b) 0 °C; (c) -30 °C ; (d) -60 °C.

Fig. S11 ¹³C NMR spectrum of tri-Zn complex **2** in CDCl₃ (25 °C).

Table S1 Selected bond length (Å) and bond angles (°) for cobalt complex **1**

Complex 1			
Co(1)-O(1)	2.001(4)	Co(1)-N(7)	2.253(4)
Co(1)-O(2)	1.936(4)	Co(1)-N(8)	2.109(5)
Co(1)-O(3)	2.040(4)		
Co(2)-O(1)	2.066(3)	Co(2)-O(7)	2.026(4)
Co(2)-O(4)	2.110(4)	Co(2)-N(1)	2.115(5)
Co(2)-O(5)	2.013(4)	Co(2)-N(11)	2.162(5)
Co(3)-O(5)	2.025(4)	Co(3)-N(15)	2.218(4)
Co(3)-O(6)	1.972(4)	Co(3)-N(16)	2.164(5)
Co(3)-O(8)	2.050(4)	Co(1)...Co(3)	5.0201(11)
O(1)-Co(1)-O(2)	135.37(15)	O(2)-Co(1)-N(7)	89.41(15)
O(1)-Co(1)-O(3)	91.53(15)	O(3)-Co(1)-N(7)	177.44(16)
O(2)-Co(1)-O(3)	92.88(15)	O(2)-Co(1)-N(8)	106.55(17)
O(1)-Co(1)-N(7)	87.64(15)	O(3)-Co(1)-N(8)	96.65(16)
O(1)-Co(1)-N(8)	116.98(17)	N(7)-Co(1)-N(8)	81.59(16)
O(1)-Co(2)-O(4)	95.60(14)	N(1)-Co(2)-O(4)	97.52(16)
O(1)-Co(2)-O(5)	96.41(14)	N(1)-Co(2)-O(5)	177.03(16)
O(1)-Co(2)-O(7)	166.47(15)	N(1)-Co(2)-O(7)	85.93(16)
O(4)-Co(2)-O(5)	80.10(15)	N(11)-Co(2)-O(1)	90.91(15)
O(4)-Co(2)-O(7)	91.98(15)	N(11)-Co(2)-O(4)	162.84(17)
O(5)-Co(2)-O(7)	95.91(15)	N(11)-Co(2)-O(5)	83.41(16)
N(1)-Co(2)-O(1)	82.00(15)	N(11)-Co(2)-O(7)	84.99(16)
N(1)-Co(2)-N(11)	99.10(17)	O(6)-Co(3)-N(16)	102.52(16)
O(5)-Co(3)-O(6)	157.15(16)	O(8)-Co(3)-N(16)	88.66(16)
O(5)-Co(3)-O(8)	93.92(15)	O(5)-Co(3)-N(15)	87.84(15)
O(6)-Co(3)-O(8)	91.75(15)	O(6)-Co(3)-N(15)	90.29(15)
O(5)-Co(3)-N(16)	99.73(16)	O(8)-Co(3)-N(15)	170.27(16)
N(15)-Co(3)-N(16)	81.61(17)	Co(1)...Co(2)...Co(3)	94.52(27)

Table S2 Selected bond length (Å) and bond angles (°) for zinc complex **2**

Complex 2			
Zn(1)-O(1)	1.9594(12)	Zn(1)-N(7)	2.2682(16)
Zn(1)-O(2)	1.9261(14)	Zn(1)-N(8)	2.1027(17)
Zn(1)-O(3)	2.0846(14)		
Zn(2)-O(1)	2.1225(13)	Zn(2)-O(7)	2.0478(13)
Zn(2)-O(4)	2.0217(13)	Zn(2)-N(1)	2.1869(16)
Zn(2)-O(5)	2.0312(13)	Zn(2)-N(11)	2.2445(15)
Zn(3)-O(5)	1.9865(13)	Zn(3)-N(15)	2.2818(15)
Zn(3)-O(6)	1.9433(13)	Zn(3)-N(16)	2.1131(16)
Zn(3)-O(8)	2.0485(13)	Zn(1)...Zn(3)	5.7310(4)
O(1)-Zn(1)-O(2)	123.63(6)	O(2)-Zn(1)-N(7)	92.37(6)
O(1)-Zn(1)-O(3)	92.55(5)	O(3)-Zn(1)-N(7)	172.63(6)
O(2)-Zn(1)-O(3)	93.10(6)	O(2)-Zn(1)-N(8)	118.08(6)
O(1)-Zn(1)-N(7)	88.53(5)	O(3)-Zn(1)-N(8)	91.57(6)
O(1)-Zn(1)-N(8)	117.75(6)	N(7)-Zn(1)-N(8)	81.49(6)
O(1)-Zn(2)-O(4)	95.37(5)	N(1)-Zn(2)-O(4)	95.25(6)
O(1)-Zn(2)-O(5)	93.45(5)	N(1)-Zn(2)-O(5)	168.54(6)
O(1)-Zn(2)-O(7)	162.94(5)	N(1)-Zn(2)-O(7)	87.31(6)
O(4)-Zn(2)-O(5)	93.25(5)	N(11)-Zn(2)-O(1)	86.57(5)
O(4)-Zn(2)-O(7)	94.76(6)	N(11)-Zn(2)-O(4)	170.98(6)
O(5)-Zn(2)-O(7)	99.65(5)	N(11)-Zn(2)-O(5)	77.83(5)
N(1)-Zn(2)-O(1)	78.12(5)	N(11)-Zn(2)-O(7)	85.57(5)
N(1)-Zn(2)-N(11)	93.77(6)	O(6)-Zn(3)-N(16)	118.36(6)
O(5)-Zn(3)-O(6)	119.10(5)	O(8)-Zn(3)-N(16)	94.43(6)
O(5)-Zn(3)-O(8)	92.51(5)	O(5)-Zn(3)-N(15)	88.04(5)
O(6)-Zn(3)-O(8)	94.53(6)	O(6)-Zn(3)-N(15)	89.61(5)
O(5)-Zn(3)-N(16)	121.22(6)	O(8)-Zn(3)-N(15)	174.92(6)
N(15)-Zn(3)-N(16)	80.99(6)	Zn(1)...Zn(2)...Zn(3)	108.98(8)

Table S3 Selected bond length (Å) and bond angles (°) for nickel complex **3**

Complex 3			
Ni(1)-O(1)	2.0626(18)	Ni(1)-N(7)	2.195(2)
Ni(1)-O(2)	2.0779(17)	Ni(1)-N(8)	2.048(2)
Ni(1)-O(3)	2.148(2)	Ni(1)-O(5)	2.0007(17)
Ni(2)-O(2)	2.1404(17)	Ni(2)-O(4)	2.0099(18)
Ni(2)-O(2A)	2.1404(17)	Ni(2)-O(4A)	2.0099(18)
Ni(2)-N(4)	2.047(2)	Ni(2)-N(4A)	2.047(2)
		Ni(1)...Ni(1A)	6.8512(6)
O(1)-Ni(1)-O(2)	169.18(7)	O(2)-Ni(1)-N(7)	93.83(7)
O(1)-Ni(1)-O(3)	87.68(7)	O(3)-Ni(1)-N(7)	175.49(7)
O(2)-Ni(1)-O(3)	88.60(7)	O(2)-Ni(1)-N(8)	94.00(7)
O(1)-Ni(1)-N(7)	90.59(8)	O(3)-Ni(1)-N(8)	90.27(8)
O(1)-Ni(1)-N(8)	96.17(8)	N(7)-Ni(1)-N(8)	85.77(8)
O(5)-Ni(1)-O(1)	81.47(7)	O(5)-Ni(1)-N(7)	89.82(8)
O(5)-Ni(1)-O(2)	88.67(7)	O(5)-Ni(1)-N(8)	174.99(8)
O(5)-Ni(1)-O(3)	94.04(8)	O(4)-Ni(2)-O(4A)	90.13(11)
O(2)-Ni(2)-O(4)	100.99(7)	O(4)-Ni(2)-N(4)	88.85(8)
O(2)-Ni(2)-O(4A)	86.73(7)	O(4A)-Ni(2)-N(4)	171.80(8)
O(4A)-Ni(2)-N(4A)	88.84(8)	O(4)-Ni(2)-N(4A)	171.80(8)
N(4)-Ni(2)-N(4A)	93.31(12)	N(4)-Ni(2)-O(2A)	87.07(7)
O(4)-Ni(2)-O(2A)	86.74(7)	N(4A)-Ni(2)-O(2A)	85.48(7)
O(4A)-Ni(2)-O(2A)	100.99(7)	N(4)-Ni(2)-O(2)	85.48(7)
O(2A)-Ni(2)-O(2)	169.13(9)	N(4A)-Ni(2)-O(2)	87.07(7)
		Ni(1)...Ni(2)...Ni(1A)	135.58(7)

Table S4 Crystallographic data of complexes **1-3**

	1 $\cdot 2\text{CH}_2\text{Cl}_2\cdot\text{C}_6\text{H}_{14}$	2	3
formula	$\text{C}_{76}\text{H}_{88}\text{Cl}_4\text{Co}_3\text{N}_{16}\text{O}_8$	$\text{C}_{68}\text{H}_{70}\text{N}_{16}\text{O}_8\text{Zn}_3$	$\text{C}_{68}\text{H}_{74}\text{Ni}_3\text{N}_{16}\text{O}_{10}$
Formula weight	1672.21	1435.57	1451.56
Temp (K)	100(2) K	100(2) K	100(2) K
Crystal system	Triclinic	Triclinic	Monoclinic
Space group	<i>P</i> -1	<i>P</i> -1	<i>C</i> 2/ <i>c</i>
<i>a</i> (Å)	14.6622(3)	15.2998(3)	31.3010(11)
<i>b</i> (Å)	15.0595(3)	16.3673(3)	14.6377(5)
<i>c</i> (Å)	19.7854(5)	16.6280(3)	21.7838(14)
α (deg)	92.9070(10)	74.5940(10)	90
β (deg)	102.128(2)	67.2980(10)	132.1870(10)
γ (deg)	114.9770(10)	62.4570(10)	90
<i>V</i> (Å ³)	3823.54(15)	3386.56(11)	7395.3(6)
<i>Z</i>	2	2	4
<i>D</i> _{calc} (Mg/m ³)	1.452	1.408	1.304
μ (Mo K α)(mm ⁻¹)	0.850	1.121	0.821
<i>F</i> (000)	1738	1488	3032
Reflections collected	66988	60723	63964
No. of parameters	976	866	451
Indep. reflns (<i>R</i> _{int})	19047(0.1169)	16763(0.0274)	9184(0.0278)
<i>R</i> 1[<i>I</i> > 2 σ (<i>I</i>)]	0.0759	0.0319	0.0285
w <i>R</i> 2 [<i>I</i> > 2 σ (<i>I</i>)]	0.1893	0.0830	0.0787
Goodness-of-fit on <i>F</i> ²	1.032	1.097	1.088

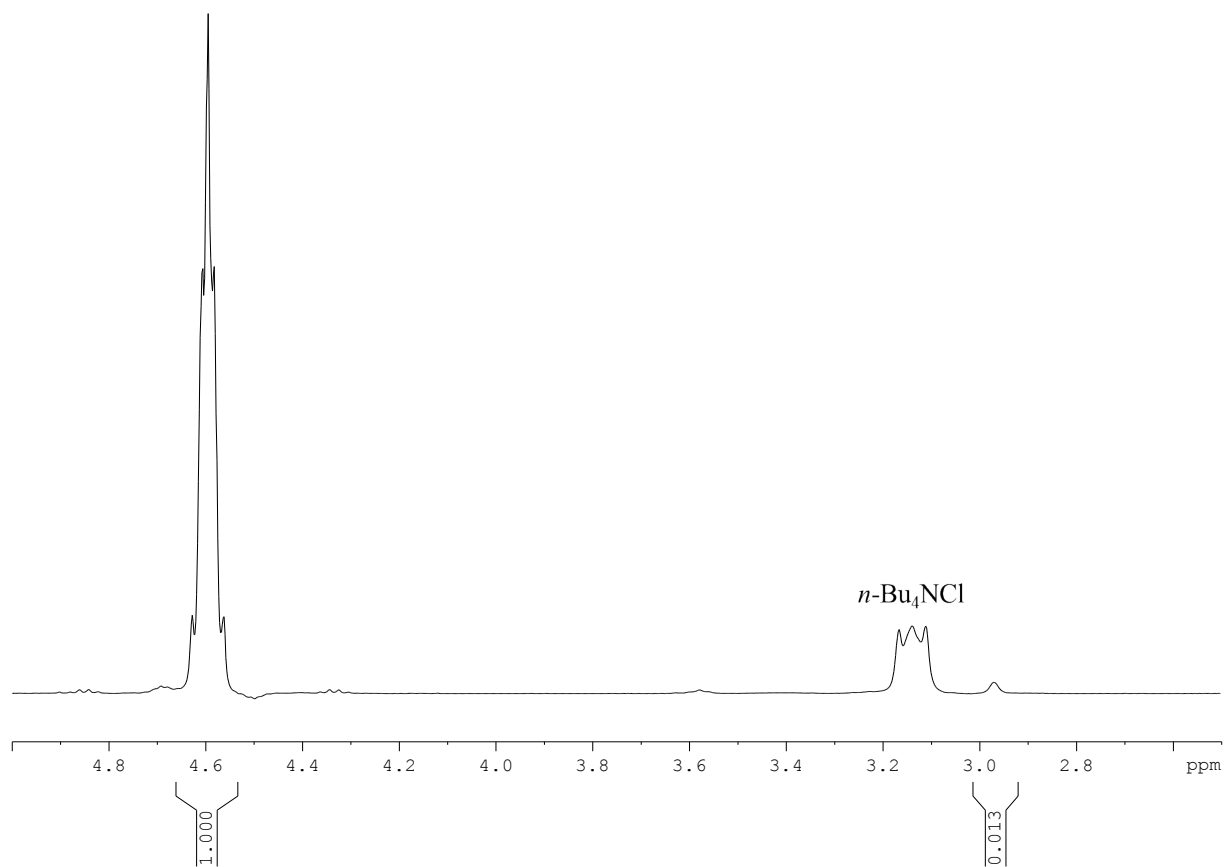


Fig. S1 ¹H NMR spectrum of the methine region of crude sample produced by coupling of cyclohexene oxide and CO₂ using cobalt acetate complex **1** in the presence of *n*-Bu₄NCl (5 mol%) at 80 °C and 300 psi CO₂ (400 MHz, CDCl₃).

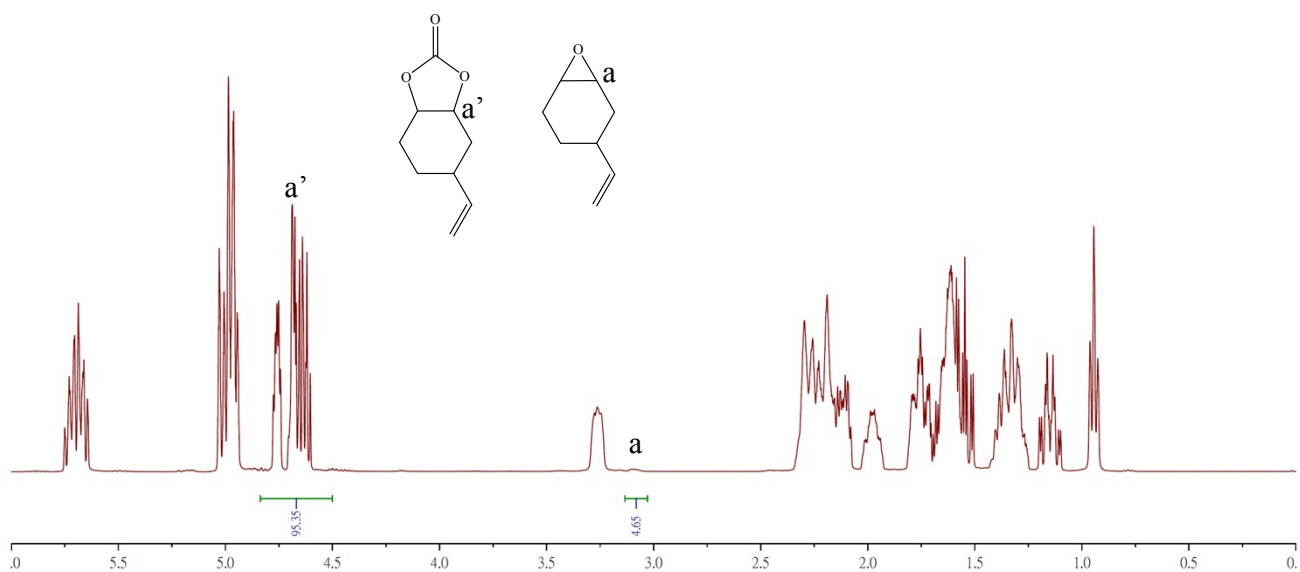


Fig. S2 ¹H NMR spectrum of the crude sample from cycloaddition of **4b** and CO₂ using tri-cobalt acetate complex **1** in the presence of *n*-Bu₄NCl.

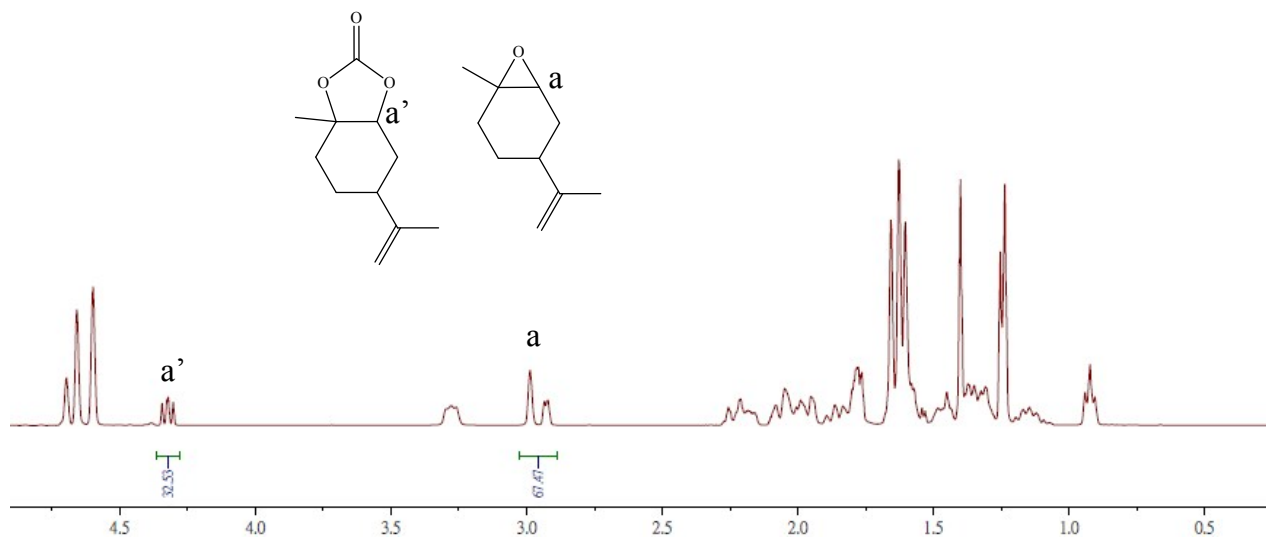


Fig. S3 ^1H NMR spectrum of the crude sample from cycloaddition of **4c** and CO_2 using tri-cobalt acetate complex **1** in the presence of $n\text{-Bu}_4\text{NCl}$.

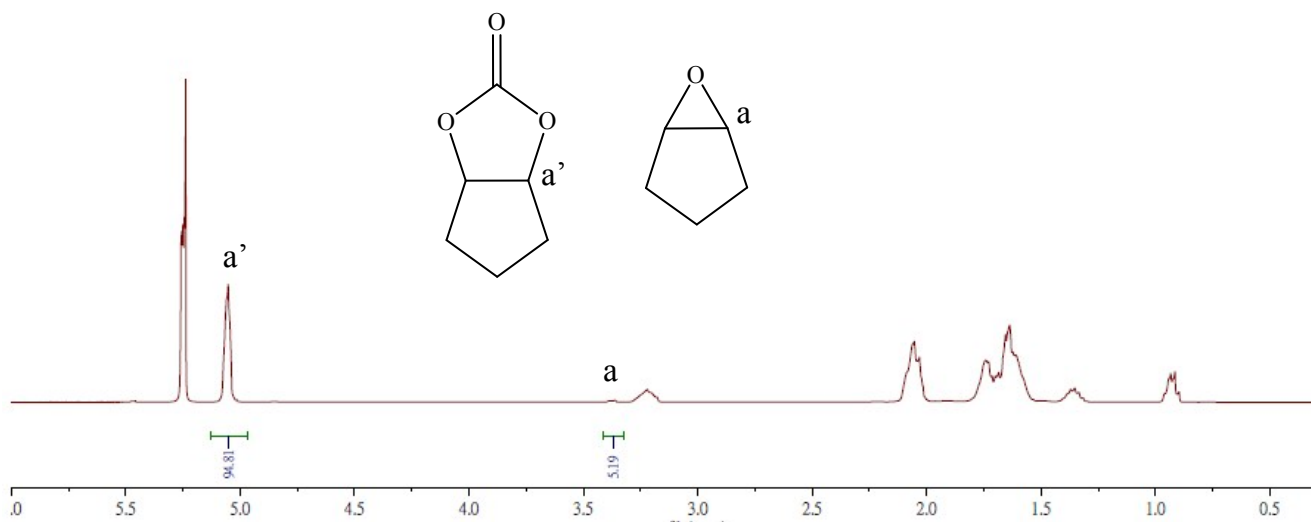


Fig. S4 ^1H NMR spectrum of the crude sample from cycloaddition of **4d** and CO_2 using tri-cobalt acetate complex **1** in the presence of $n\text{-Bu}_4\text{NCl}$.

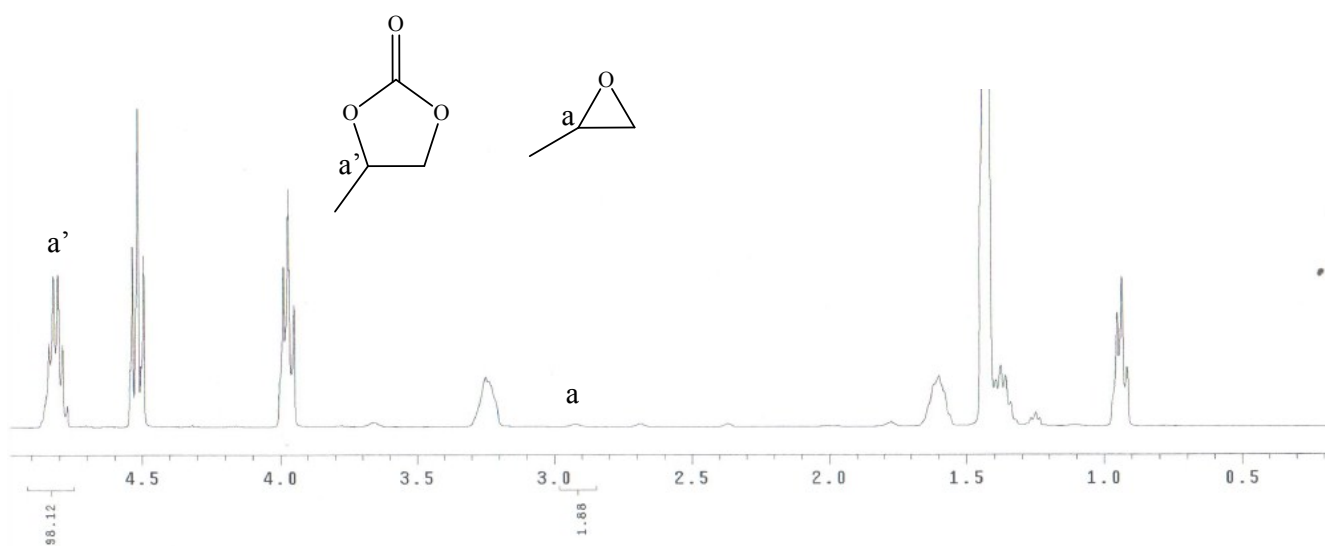


Fig. S5 ¹H NMR spectrum of the crude sample from cycloaddition of **4e** and CO₂ using tri-cobalt acetate complex **1** in the presence of *n*-Bu₄NCl.

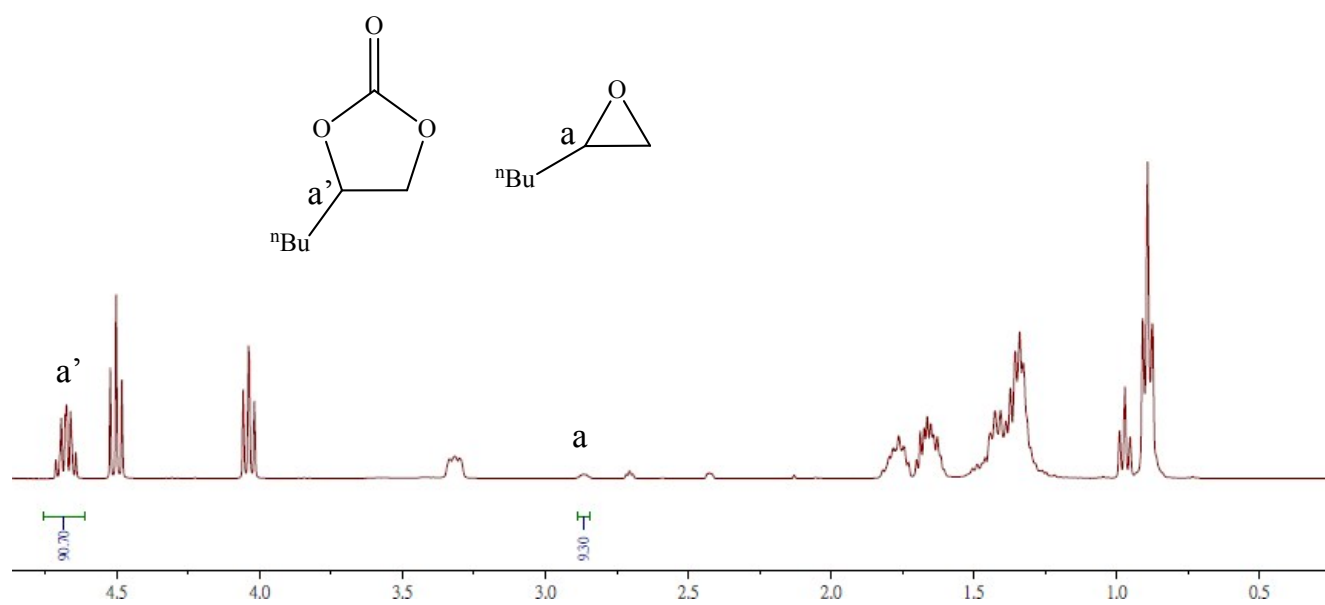


Fig. S6 ^1H NMR spectrum of the crude sample from cycloaddition of **4f** and CO_2 using tri-cobalt acetate complex **1** in the presence of $n\text{-Bu}_4\text{NCl}$.

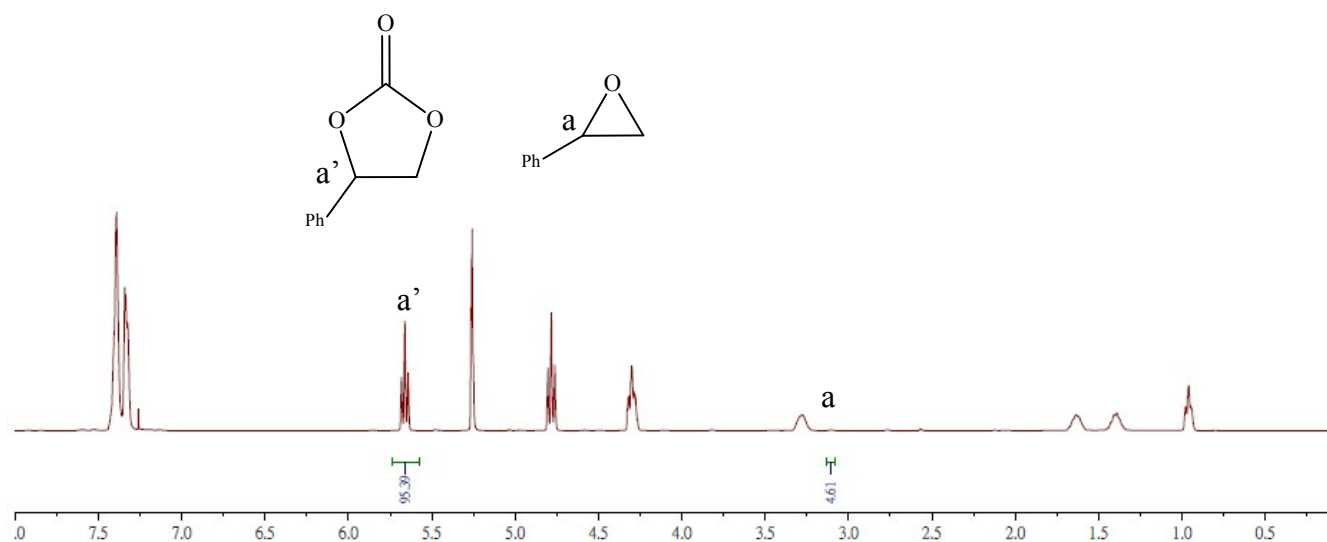


Fig. S7 ¹H NMR spectrum of the crude sample from cycloaddition of **4g** and CO₂ using tri-cobalt acetate complex **1** in the presence of *n*-Bu₄NCl.

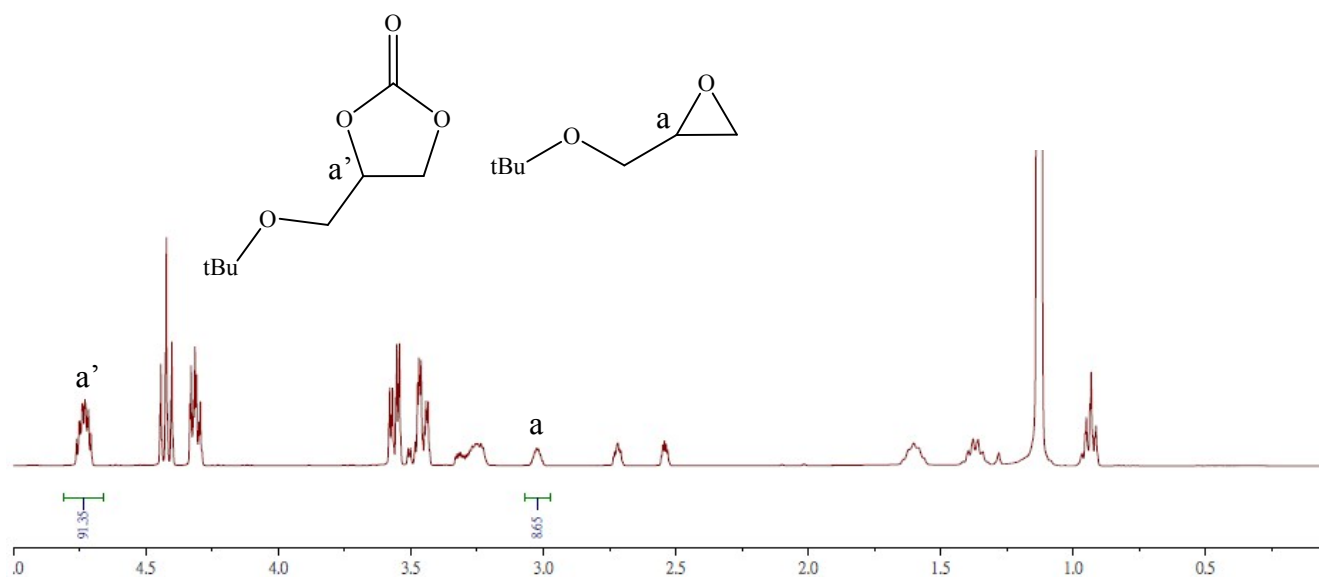


Fig. S8 ¹H NMR spectrum of the crude sample from cycloaddition of **4h** and CO₂ using tri-cobalt acetate complex **1** in the presence of *n*-Bu₄NCl.

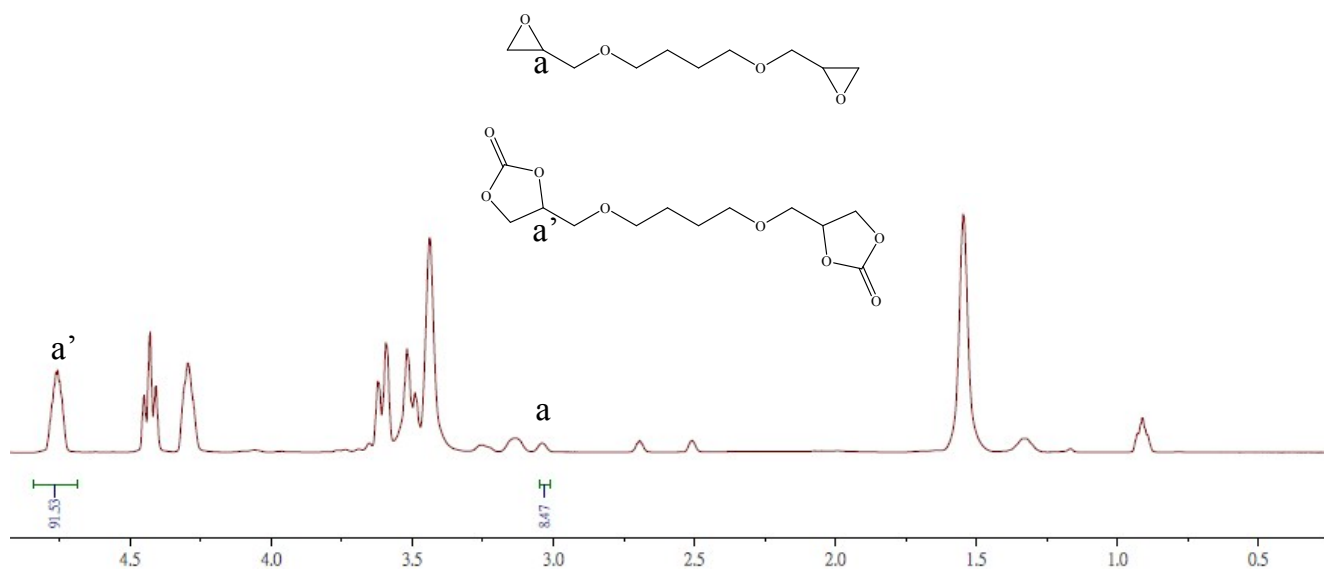


Fig. S9 ¹H NMR spectrum of the crude sample from cycloaddition of **4i** and CO₂ using tri-cobalt acetate complex **1** in the presence of *n*-Bu₄NCl.

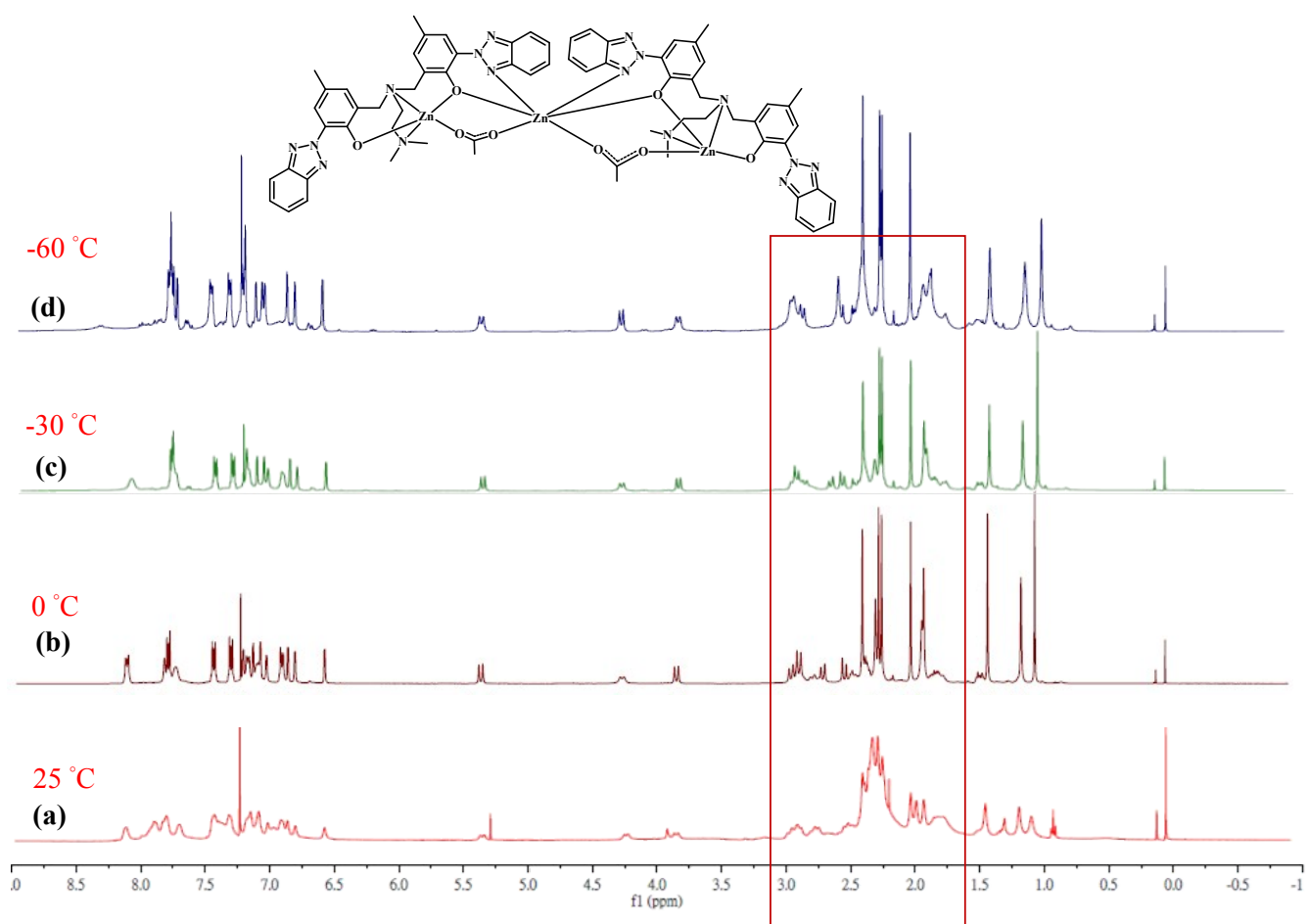


Fig. S10 Variable-temperature ¹H NMR spectrum (400 MHz) of tri-Zn complex **2** in CDCl₃ taken at different temperatures: (a) 25 °C; (b) 0 °C; (c) -30 °C ; (d) -60 °C.

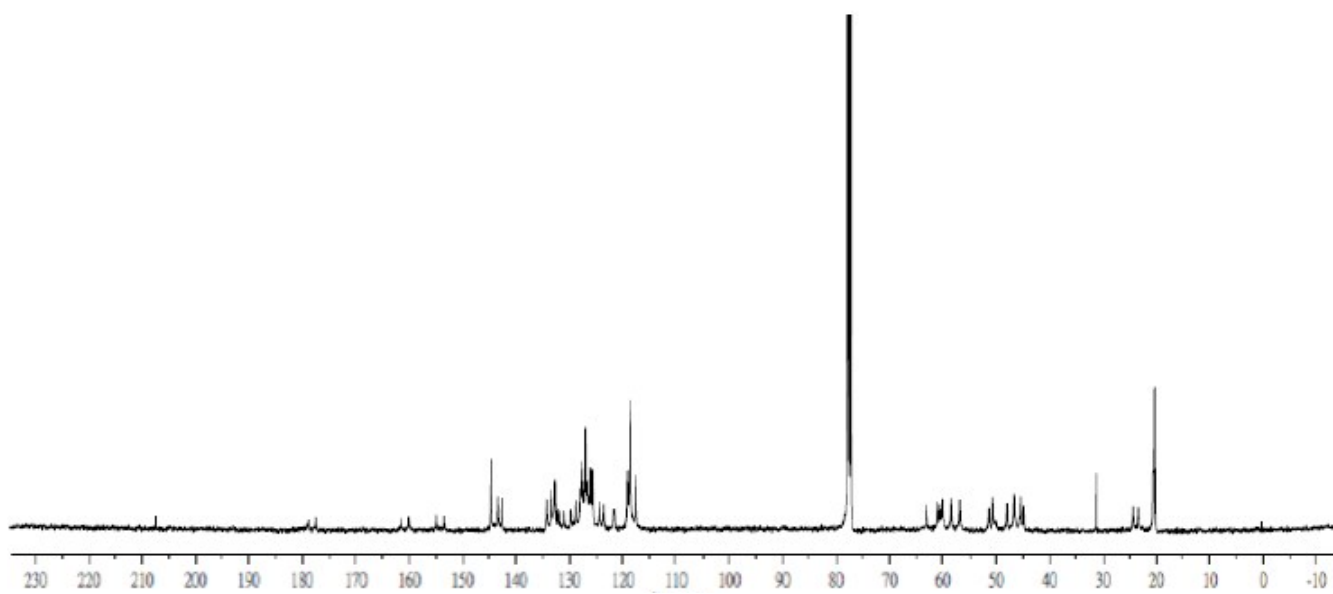


Fig. S11 ^{13}C NMR spectrum of tri-Zn complex **2** in CDCl_3 (25 °C).